

Free-Roaming Planar Motors: Toward Autonomous Precision Planar Mobile Robots

T. B. Lauwers, Z. K. Edmondson, and R. L. Hollis

The Robotics Institute

Carnegie Mellon University

Pittsburgh, Pennsylvania, USA

tlauwers@andrew.cmu.edu, zke@andrew.cmu.edu, rhollis@cs.cmu.edu

Abstract—We present what we believe to be the first free-roaming planar motors. Unlike conventional planar motors requiring a tether for air, power, and signals, these planar motor forcers are tetherless and self-contained. We have designed and operated such forcers utilizing both mechanical bearings and air bearings with air supplied by an on-board pump. Considerations of on-board power, bearing means, wireless communications, and systems integration are discussed in the paper. Performance results for the air bearing model are reported, and work needed to develop future practical autonomous precision planar mobile robots based on tetherless planar motors is given.

I. INTRODUCTION

Imagine a mobile robot which could move over arbitrarily large distances in the plane at speeds of the order of a meter per second, yet be able to position itself with sub-micrometer motion resolution. Further, imagine that this robot is essentially an ideal frictionless mass with a single moving part. This paper describes efforts to produce such a robot based on the concept of a free-roaming planar motor.

Considerably ahead of his time, Bruce Sawyer in 1968 [1] introduced the concept of the planar motor, commonly referred to nowadays as the “Sawyer” motor. This motor provides motion in the plane (and limited rotation), thereby eliminating the need for stacked linear stages to provide orthogonal degrees of freedom.

Figure 1 illustrates the operating principles. In Fig. 1(a), the planar motor is shown consisting of a moving *forcer* and a stationary *platen* or stator surface. The forcer rides over the platen on an air bearing film, typically 10-15 μm thick, and can carry a payload along an arbitrary planar path from point A to point B. The platen surface is covered by a dense array of steel teeth (typically .020 in. square on a .040 in. pitch), planarized by epoxy backfill. The forcer has a *tether* supplying air and motor currents from external sources. Figure 1(b) shows the underside of the forcer, where a pair of x linear motor segments and a pair of y linear motor segments provide balanced orthogonal forces or torque. Each of the linear motor segments operates on a well-known stepper motor principle (see Sec. II-B).

Planar linear motors have many distinct advantages, including two (and limited third rotational) degrees of freedom achieved with a single moving part, parallel rather than serial

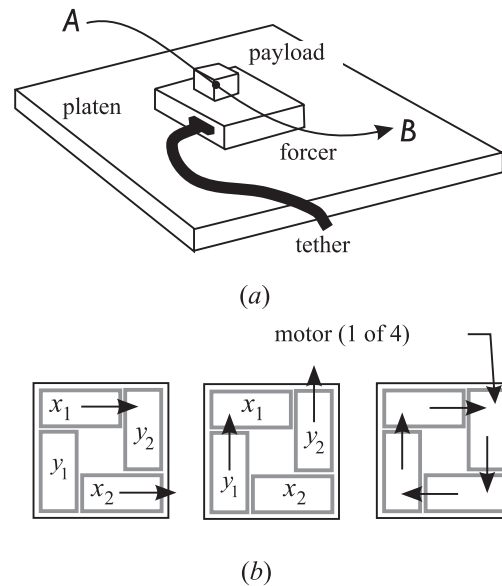


Fig. 1. Planar Motor: (a) forcer moving on air bearing over a platen (stator), (b) bottom view of forcer showing four motor sections providing force and torque.

kinematics, frictionless operation, direct coupling to mechanical “ground,” high precision, large workspace, and the ability to operate multiple forcers on a single platen surface.

On the other hand, currently available planar linear motors are severely limited because of their open-loop stepping operation which prevents the achievement of maximum potential performance. To help ensure against loss of synchrony (missing steps), only two-thirds to three-fourths of the available force margin is used, reducing the forcer’s potential maximum acceleration and velocity. Even so, the forcer motors remain susceptible to loss of synchrony if large enough unanticipated external forces are acting. Additionally, settling times after moves are longer than desirable and there is no way to reject low-frequency external disturbances. The forcer has only moderate stiffness requiring high power dissipation when holding a position. Finally, the need to provide air and power through a tether connection complicates motion planning [2] and is a serious drawback for many applications (the concern of this paper).

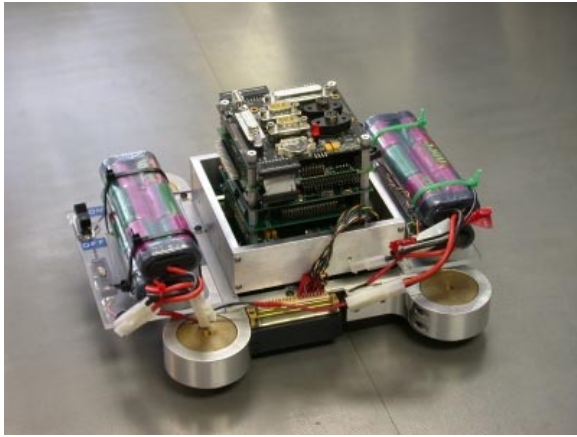


Fig. 2. Tetherless planar motor forcer using four ball wheels for support.

II. EXPERIMENTAL FREE-ROAMING PLANAR MOTORS

We have endeavored over the past several years to evaluate methods that could be used to free the planar motor forcer from the restrictions of having a tether. Several barriers must be overcome to achieve this goal:

- *Energy:* Some way to soak up energy from the environment or store energy on-board must be found. Methods must be found to increase efficiency to minimize power consumption.
- *Bearings:* Externally-supplied air for the air bearing must be supplied on-board, through the platen surface, or alternative bearing means must be found.
- *Communication:* Wireless communication with the outside world must be implemented.
- *System Integration:* The bulky and heavy controller and drive amplifiers associated with current planar motor systems must be reduced in size and weight to fit on board.

This paper discusses our ongoing attempt to deal with these issues, presents results obtained to date with two different tetherless motors, and outlines considerations for future work we believe will lead to practical autonomous precision planar robots.

A. Tetherless planar motors with wheels

Figure 2 shows a tetherless planar motor developed in our laboratory. It was based on a modified commercial forcer from Normag, Inc. The central area of the forcer was machined out to provide space for a 3-DOF ac-magnetic position sensor with resolution of $0.2 \mu\text{m}$ (1σ) [3]. In lieu of air bearings, the forcer was fitted with a commercial 25.4 mm diameter ball wheel in each of its corners. Pulse-width modulation (PWM) drive electronics was designed and fabricated to replace the commercial off-board drive system. The on-board control system was implemented using an embedded PC platform with PC/104 form factor. Power was provided by a battery with 24 NiMH cells.

Whereas it is possible that the wheeled configuration could be designed to work well, there are several drawbacks to

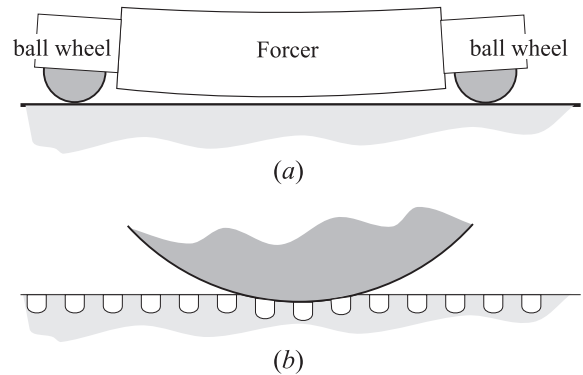


Fig. 3. Problems with ball wheels (exaggerated): (a) forcer body bowing due to magnetic preload, (b) magnified schematic of platen surface embossing due to Hertzian contact.

this approach. In particular, the ball wheels proved difficult to adjust due to flexing of their mounts and forcer housing under the forcer’s strong magnetic preload. (As a rule of thumb, each motor segment produces an attractive force that is about 10 times its lateral thrusting force. For the Normag forcer, the total attractive force is about 1000 N.) As shown in Fig. 3(a), when the ball height was adjusted using precision shims to raise the forcer by several μm above the platen surface at its center, the air gap at its edges was large enough to severely decrease the available thrust forces, leading to low accelerations. It would be possible to greatly reduce this effect by redesigning the forcer layout to incorporate the ball wheels at substantially inboard locations.

In operation, the ball wheels also caused slight embossing of the platen surface as illustrated in Fig. 3(b). The platen teeth are magnetically soft, and therefore also mechanically soft, whereas the ball wheels are made of hard steel. The planarizing epoxy backfill is also rather soft. The embossing could lead to platen wear, work hardening, and other undesirable effects. It could be reduced by incorporating a hard filler material such as Al_2O_3 into the backfill. Additionally, the ball wheels could be replaced by caster wheels having a large crown radius, although changing direction would result in some undesirable “skidding.” Finally, it is thought that the small but finite amount of rolling and static friction associated with mechanical wheels and their bearings would doubtless lead to a decrease in precision.

The above considerations notwithstanding, the tetherless wheeled forcer operated successfully on commercial English-unit platen surfaces at speeds of up to 0.2 m/s while giving us a research platform for evaluating design tradeoffs.

B. Tetherless planar motors with on-board air pump

Our second tetherless forcer, shown in Fig. 4, was designed and built “from scratch” in our laboratory at Carnegie Mellon University [4]. Its motors have approximately 30% higher force per unit area than the commercial motors, it incorporates an improved ac-magnetic position sensor (estimated resolution 100 nm , 1σ), and has an air bearing design that is approximately 10 times more efficient than the commercial motor

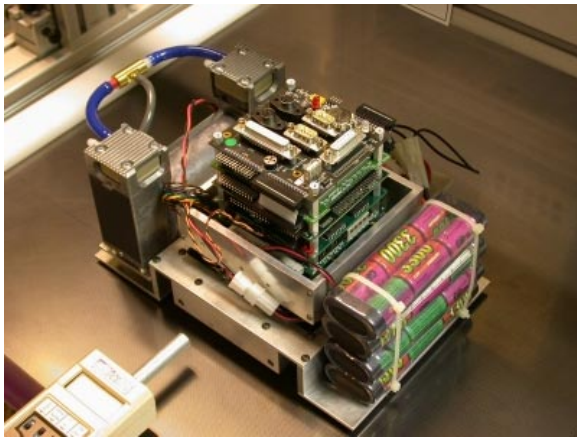


Fig. 4. Tetherless planar motor forcer using an air bearing for support with on-board pump. The device shown in the lower left of the photograph is a force measuring instrument.

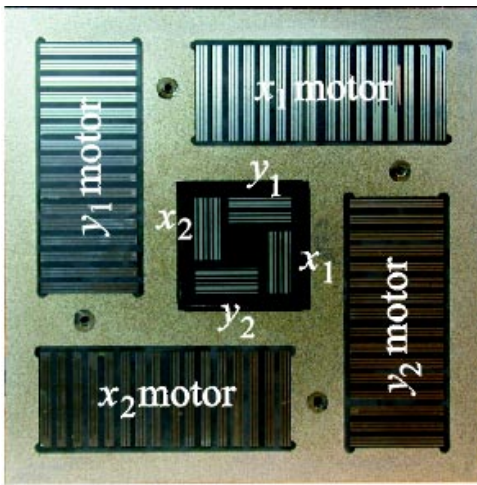


Fig. 5. Photograph of the active surface of the new forcer showing its four motors, 3-DOF ac-magnetic position sensor, and air bearing orifices [4]

making it feasible to use an on-board pump supplying air. The motor operates on an ensemble of new metric-unit platen tiles fabricated in our laboratory (Sec. III). Figure 5 is a photograph of the active surface of the forcer, measuring 137 mm square.

Figure 6 sketches the (well known) operating principle of each motor in our new tetherless planar motor. In each of the left and right parts of the motor, a NdFeB permanent magnet provides flux through SiFe laminations and the ultralow carbon steel platen surface. This flux is approximately half that required for magnetic saturation. Each of the 8 motor poles has 3 teeth, and both the motor and platen teeth have a pitch of 1.000 mm. As the windings are energized, they induce additional flux, shown by the looping arrows in Fig. 6, that either adds or subtracts from the permanent magnet flux, depending on the pole in question. At maximum current, the fluxes will add to saturate one pole, while the adjacent pole will have almost zero flux. Poles with maximum flux will line up in a minimum energy configuration. As winding currents vary, the motor teeth will move relative to the platen teeth. The

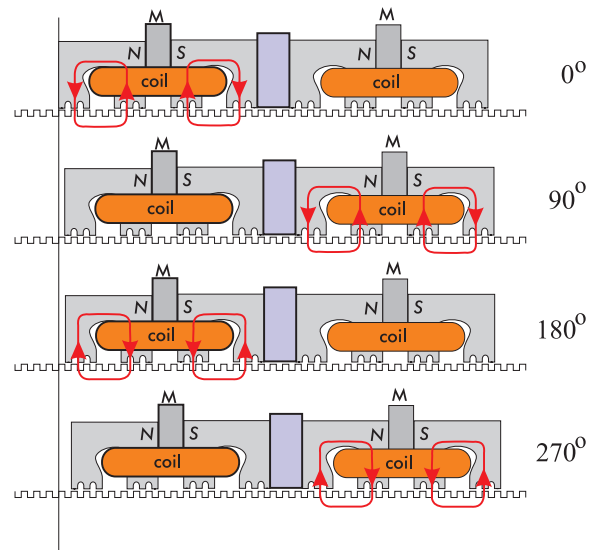


Fig. 6. Flux-steering operating principal of each motor.

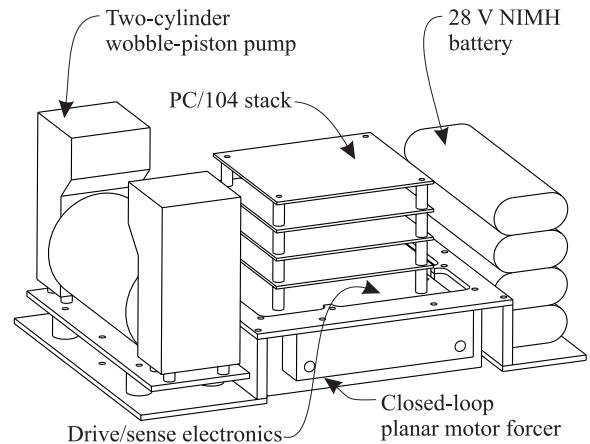


Fig. 7. Tetherless forcer design with on-board air pump.

figure shows the motor windings energized at 90° intervals through a complete 360° electrical cycle, which will advance the motor by one tooth pitch. In our design, a pair of such motors operating together forms each of the x motors and each of the y motors shown in Fig. 5.

Figure 7 shows the overall configuration of the tetherless forcer with onboard air pump. System components are built around the closed-loop planar motor forcer. Four 7V 3.3 Ah NiMH batteries are used to supply motor currents, pump currents, and power for the on-board computer. A Thomas model 8009-1067 two-cylinder wobble piston pump mounted on vibration isolators supplies the forcer air bearing. The eight phases of the motor drive uses a custom circuit board with National LMD18245 3A, 55V DMOS full bridge PWM motor drivers operated in analog input mode using the device's DAC reference voltage input. Two additional LMD18245s power the on-board air pump.

Our initial PC/104 computer was a low-power (7W) 100 MHz MZ104 CPU from Tri-M Systems. We later switched to

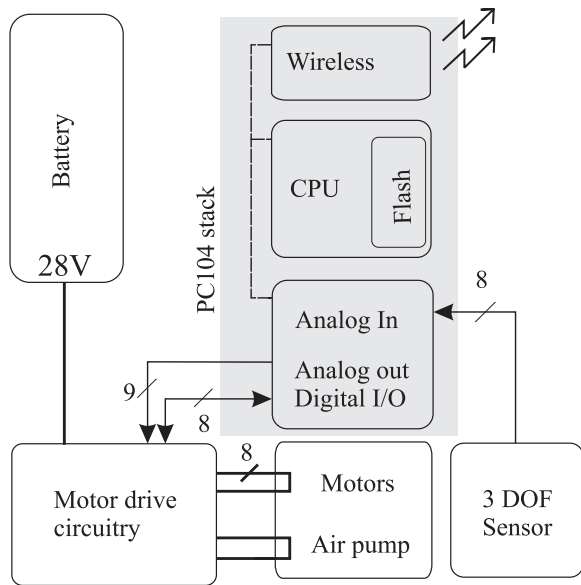


Fig. 8. System block diagram of tetherless forcer design with on-board air pump.

a Lippert GmbH 300 MHz Cool RoadRunner II with Geode GX1 processor, 256 Mb of SDRAM, 96 Mb of compact flash storage, and a PC/104-plus bus. The PC/104 stack includes the Ruby-MM 12-bit 8 channel D/A board from Diamond Systems providing voltage outputs for the motor drivers; a Diamond-MM-AT 12-bit 16 channel A/D board from Diamond Systems receiving input from the 3-DOF ac-magnetic position sensor, with auxiliary D/A outputs for the pump drive; and an Aeon PCM-3115B PCMCIA carrier board for an Orinoco 802.11b wireless adapter for communication. The PC/104 stack consumes only about 7.25 W with the MZ104 board and about 15 W with the Lippert board. Fig. 8 shows the relationships between system components.

The QNX 6.1 real-time operating system was used on the PC/104 platform with a custom subset of QNX installed on board. The operating system, programs, and data take up about 10 MB and are stored on a DiskOnChip flash memory on the MZ104 board. Sine- and cosine-waves for microstepping the motor are generated by a table lookup scheme enabling an update rate of 3.33 KHz, even on the relatively slow processor.

The mass M of the tetherless forcer with on-board air pump is 6.91 Kg. Of this mass, the pump is 2.24 Kg, the 24 cells of the NiMH battery are 1.58 Kg, the PC/104 stack is 0.57 Kg, the PCM drivers and heat sink is 0.83 Kg, miscellaneous hardware is 0.74 Kg and the forcer itself is 0.95 Kg. The forcer has been tested with loads of up to 23 Kg which the air bearing can easily support. The magnetically-preloaded air bearing is remarkably stiff, measuring about $88 \text{ N}/\mu\text{m}$ using laser interferometry. The peak forcer thrust F_x or F_y is approximately 28 N at 2.5 A per phase. Thus the maximum possible acceleration is $a = F/M = 4.05 \text{ ms}^{-2}$. (If the forcer moves in a 45° diagonal, the maximum acceleration increases by $\sqrt{2}$.)

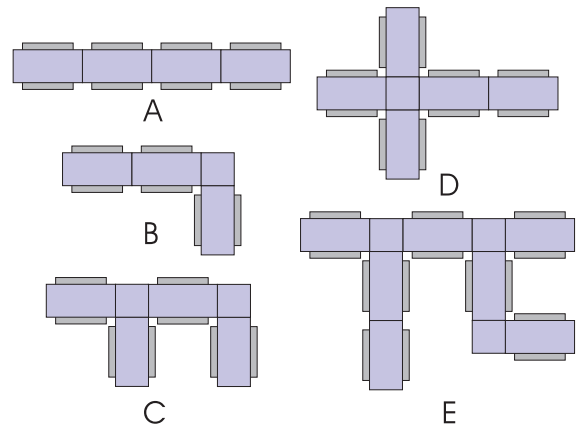


Fig. 9. Various platen tile configurations. Rectangular platens are joinable on their short sides to form arbitrarily long “highways” for planar motor forcers.

III. FIELD-JOINABLE PLATEN TILES

Tethered planar motor forcers, because of their finite tether lengths, necessarily have a restricted motion range. Additionally, manufacturing considerations limit the size of platens; for example, standard commercial platens are available in sizes up to 37 in. \times 52 in. (940 mm \times 1321 mm). On the other hand, untethered free-roaming forcers can potentially travel over much larger areas.

To help solve this problem, we have produced platens with continuous surfaces composed of contiguous modular *field-joinable tiles*. The tiles can be flexibly arranged in various ways to form *platen ensembles* providing continuous stators for multiple free-roaming forcers [5]. Our platen tiles are either rectangular, 1200 mm \times 600 mm, or 600 mm square. Rectangular tiles have a mass of 77 Kg and feature a planarized array of 720,000 square ferromagnetic posts on a 1 mm pitch. The post array provides electromagnetic reaction forces for the forcer’s motors, and also act as position references. The tiles are light enough to be handled by two persons, and are supported on bases by a series of precision leveling screws and locating fixtures. As illustrated in Fig. 9, square tiles are used in conjunction with the rectangular tiles to form precise and level platen ensembles with L-junctions, X-junctions and T-junctions to support a variety of layouts. Figure 10 is a photograph of a section taken at a T-junction formed by three rectangular tiles and one square tile. Worst case height misalignments at tile junctions are approximately $5 \mu\text{m}$, permitting forcers to travel over the interface crack at typical altitudes of 10-15 μm . The tiles are joined and unjoined using specially-developed mechanisms. Square tiles need no support. Tiles are fitted with modular UHMW polyethylene curbs providing boundaries for forcer operation.

IV. EXPERIMENTAL RESULTS

Several measurements were made of forcer motor force vs. position relative to the platen teeth at various currents to determine the relative permeance function. Additionally, forcer motor “pullout” tests were performed to measure the

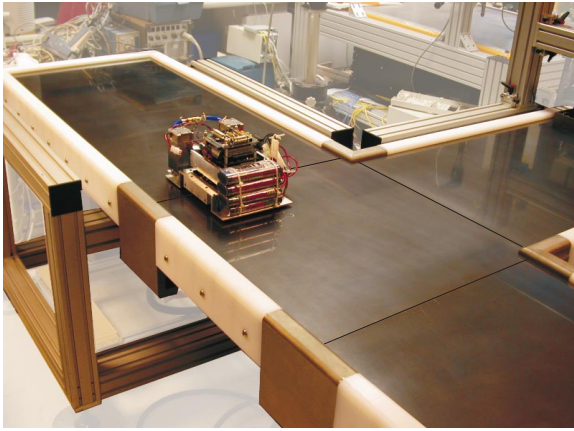


Fig. 10. Photograph of a T-junction between three rectangular platen tiles and one square platen tile. (The interface cracks between tiles are emphasized for clarity.)

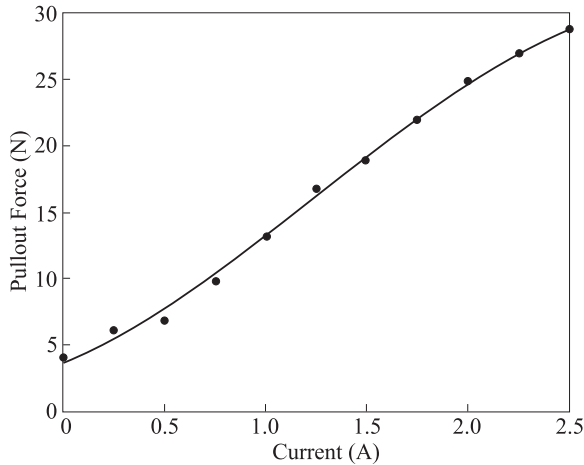


Fig. 11. Typical forcer x - or y -direction force output vs. drive current.

peak force required to lose synchrony (skip platen teeth) as a function of motor current. Figure 11 shows typical results for equal currents in both phases, *i.e.*, 45° phase angle (*cf.* Fig. 6). Results show a forcer output of 28 N (6.3 lb.) at 2.5 A, with only slight saturation rolloff.

A number of air bearing tests were performed on the tetherless forcer with on-board air pump. Figure 12 shows forcer flying height vs. pump power, measured by laser interferometry. The scatter in data points is thought to be due to pump vibration, and the curve is meant to show the general trend. Liftoff occurs at about 20 W, but substantial power is required to fly at higher altitudes. At least 60 W is required to cross over the $\sim 5 \mu\text{m}$ worst case misalignments between platen tiles (Sec. III).

We also performed a number of tests to determine maximum achievable accelerations and velocities. These tests were performed in open-loop mode as the closed-loop sensing and control functions for the tetherless forcer are not yet operational. Reliable maximum accelerations of 0.4 ms^{-2} at low speeds and 0.55 ms^{-2} at higher speeds was achieved. Experiments

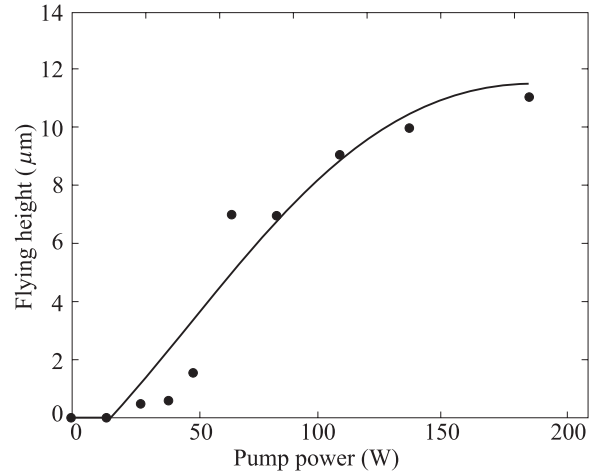


Fig. 12. Forcer flying height vs. pump power.

occasionally measured accelerations as high as 2.1 ms^{-2} , but usually resulted in missed steps. These values are considerably lower than the theoretical maximum of 4.05 ms^{-2} . Work is ongoing to explore these limits. Reliable maximum speeds of 0.55 m/s were achieved, compared with about 1.5 m/s for an open-loop tethered forcer operating at 160 V, and 2.0 m/s for a closed-loop tethered forcer operating at 160 V [6], [7]. The tetherless performance is limited both by the lower 28 V drive voltage and the reduced 100-300 MHz computational speed compared with tethered forcers having off-board power and computational resources.

To execute a move, the on-board computer sends sine- and cosine-wave drives to the motors, with frequencies ramped up during the acceleration phase, and ramped down during deceleration to avoid skipping platen teeth. The average power usage during maximum speed moves was determined from the RMS values of the waveforms to be 63 W for the forcer axis being driven, plus a DC voltage resulting in 15 W dissipation for the orthogonal axis needed to stabilize the trajectory, 108 W needed for the on-board pump, and 15 W needed for the on-board computer for a total of 201 W. Since the batteries can store only about 90 W-hrs, running time is limited to about 27 minutes.

Power consumption is dominated by the on-board pump. During the course of the work, two different smaller and less power-hungry air pumps made by Thomas were tried but found to be marginally insufficient for providing the correct combination of air pressure and flow for the air bearing.

In one test, the tetherless forcer successfully made 70 round trip motions of 1.72 m each for a total distance of 120 m on a battery charge lasting about 12 minutes. In another test, the tetherless forcer successfully moved over distances of about 3.5 m at maximum speed, repeatedly crossing the boundaries between a set of four platen tiles.

V. CONCLUSIONS

We have demonstrated successful operation of two different tetherless planar motor forcers. The first used a modified

commercial forcer with ball wheels for support and operated on a commercial platen. The second used a new custom-made forcer with air bearing supplied by an on-board pump, operating on an ensemble of custom-made platen tiles. Performance measurements were made concerning motor forces, the air bearing, power consumption, battery life, maximum accelerations, and maximum velocities.

New, field-joinable platen tiles were introduced, providing a special operational “floor” for planar robots, allowing untethered forcers to roam freely over arbitrarily long distances.

Elimination of the planar motor forcer’s tether immediately suggests important advantages, but this goal has proved to be illusive. We have concluded that the forcers we have so far developed are not practical. The ball wheels have severe drawbacks as pointed out in Sec. II-A. The on-board pump has the drawback of excessive power consumption and excessive vibration. Nevertheless, both tetherless forcers were demonstrated to work. We believe this is the first such demonstration of free-roaming planar motors.

Despite our somewhat negative assessments, we remain optimistic about the eventual practicality of tetherless planar motors, and project that they can one day form the basis for precise and versatile free-roaming planar robots that can be used in a wide variety of important applications.

VI. FUTURE WORK

Much work remains to be done. The first order of business is to solve the air bearing problem. There is really no viable substitute for the air bearing, wheeled forcers notwithstanding. The solution is to deliver high-pressure air through the platen surface. At first blush it would seem that just drilling an array of holes in the platen surface and supplying air in the manner of an air hockey table would work. This is not the case because of the strong magnetic preloading (~ 1000 N) of the forcer’s motors. (Air would simply escape through all the holes not covered by forcers. Moreover, this would constitute an unrealistic combination of air volume and pressure, requiring an extremely large compressor.) What is needed are air valves that turn on only when covered by a forcer. While the valves could in principle be actively controlled, this would be needlessly complicated when multiple forcers are used on a platen. A solution that uses an array of passively operated microvalves would be ideal. Approximately 1000 to 1600 valves per square meter of platen surface will suffice. There are formidable design and manufacturing challenges associated with this approach which we are just beginning to explore. If this approach can be made to work and be made practical, power-hungry and heavy on-board pumps can be eliminated.

We are currently operating the tetherless forcer in open-loop microstepping mode. Incorporate sensing and feedback as we have done in our previous closed-loop tethered forcers will greatly reduce power consumption. It has been shown that operating in closed-loop mode requires only about one-eighth of the power as open-loop mode for typical series of moves [7]. If the air bearing problem is solved, and closed-loop operation is implemented, the next step might be to

extend the time between rechargings by moving to state-of-the-art available Li-ion batteries which have 30% greater energy density than the NiMH batteries. Small direct methanol fuel cells developed for laptop computers would be another option to consider. Also, the PC/104 stack can be reduced to a single board implementation, saving on power, volume, and weight.

With the improvements noted above, total power consumption should drop dramatically, allowing operation of up to 6 hours between rechargings. The reduced weight would allow higher accelerations, and the physical size would be only marginally larger than that of a conventional tethered forcer. It is likely that inductive recharging techniques can be used for the on-board batteries. Refueling stations could be used for fuel cells. Additional sensing and actuation subsystems could be carried on top of the forcer. These modifications would set the stage for adding a great deal of functionality to the tetherless forcer, effectively creating a versatile and precise planar robot.

Autonomous precision planar robots based on tetherless closed-loop planar motor forcers would constitute a new class of mobile robots. Fleets of such robots could be readily deployed on “factory floors” comprised of contiguous arrangements of passive modular platen tiles. Such robots could precisely move small samples or products over many meters of space, interacting with each other and with fixed processing and analyzing stations. Their projected motion resolution of 100 nm (1σ) is sufficiently precise to enable the realization of many important industrial applications such as gene chip production, drug discovery, chemical synthesis and analysis, biological assay, microassembly, MEMS packaging, and others.

ACKNOWLEDGMENT

The authors gratefully acknowledge the contributions of Amoury Rolin, Arthur Quaid, Rob Schlender, and Al Rizzi. The project was supported in part through National Science Foundation grants DMI9523156, DMI9527190, and DMI9900165.

REFERENCES

- [1] W. E. Hinds and B. Nocito, *Theory and Application of Step Motors*, ch. 15: The Sawyer Linear Motor, pp. 327–340. St. Paul, West Publishing Co., 1974.
- [2] S. Hert and V. Lumelsky, “The ties that bind: Motion planning for multiple tethered robots,” in *Proc. of the IEEE Int’l Conf. on Robotics and Automation*, pp. 2734–2741, May 1994.
- [3] Z. Butler, A. A. Rizzi, and R. L. Hollis, “Integrated precision 3-DOF position sensor for planar linear motors,” in *IEEE Int’l Conf. on Robotics and Automation*, (Leuven, Belgium), pp. 3109–3114, May 1998.
- [4] R. L. Hollis, A. A. Rizzi, A. E. Quaid, Z. J. Butler, and M. L. Chen, “A precision planar robot for industrial applications.” (In preparation).
- [5] R. L. Hollis, “Field-joinable platen tiles for planar linear motors.” U. S. Patent #6,545,375, April 8 2003.
- [6] A. E. Quaid and R. L. Hollis, “3-DOF closed-loop control for planar linear motors,” in *IEEE Int’l Conf. on Robotics and Automation*, (Leuven, Belgium), pp. 2488–2493, May 1998.
- [7] A. E. Quaid, *A Planar Robot for High-Performance Manipulation*. PhD thesis, Carnegie Mellon University, 2000.